INELASTIC CYCLIC RESPONSE OF CIRCULAR CORRODED CONCRETE BRIDGE PIERS

M.M. Kashani[1]

University of Southampton, Southampton, United Kingdom, mehdi.kashani@soton.ac.uk

Abstract: *This paper provides a summary of previous experimental tests on corrosion damage circular concrete bridge piers subject to lateral cycling loading. In addition, the experimental results of a recent experimental testing were conducted on corroded circular concrete bridge piers with pitting corrosion are also presented. In this research, a set of experimental tests on three reinforced concrete (RC) columns subjected to lateral cyclic loading. The columns varied in terms of corrosion presence and different reinforcement configurations. One column was meticulously reinforced to emulate modern RC bridge piers designed per current seismic codes. The second column, identical in design but affected by corrosion, represented damaged structures. The third column, minimally reinforced and corroded, simulated aging RC bridge piers not complying with contemporary seismic codes. The study revealed that corrosion significantly reduced ductility in the tested columns, surpassing the impact on their strength. Surprisingly, even the uncorroded column, designed according to current seismic codes, exhibited severe inelastic buckling of its vertical bars during cyclic tests.*

1. Introduction

Bridges stand as pivotal components within any transportation infrastructure network, their disabling capable of causing significant disruptions across the entire system. Particularly alarming are the numerous ageing major bridges still operational in earthquake-prone regions, posing a substantial challenge to their safety and functionality (ASCE, 2013; Ghosh and Padgett, 2010). To address this concern, it is imperative to systematically assess the safety, functionality, and service life of bridges through a rigorous mathematical approach.

Reinforced concrete (RC) bridges, especially those aging, are vulnerable to environmental stressors like chloride-induced corrosion and carbonation. Among these, chloride-induced corrosion of reinforcing steel emerges as a major concern affecting the performance of RC bridges in the UK, USA, and other developed countries (Rao et al., 2016a; Chiu et al., 2015). Severe corrosion can lead to catastrophic failures, resulting in significant financial burdens for countries like the UK and the US. Researchers have diligently explored the impact of corrosion on the nonlinear behaviour of structural components, shedding light on issues such as loss of reinforcement cross-section, changes in mechanical properties, and reduced compressive strength of concrete covers (Vu et al., 2016). Corrosion-induced mechanical damage affects not only individual elements but also weakens the overall structural system, highlighting the critical need for comprehensive research in this area (Kashani et al, 2016; Dizaj et al., 2021; Dizaj and Kashani, 2002; Dizaj et al. 2023).

Recent studies have delved into the influence of corrosion on seismic performance, fragility, and life-cycle cost analysis of deteriorating structures and bridges. These studies, utilizing advanced tools like OpenSees (McKenna, 2011), have emphasized the significant impact of corrosion on the seismic vulnerability of RC structures and bridges (Stewart, 2004; Choe et al., 2008; Berto et al., 2009; Akiyama et al., 2011; Alipour et al., 2011; Ou et al., 2013). However, a notable research gap exists concerning the nonlinear cyclic behaviour of circular corroded RC columns, a common feature in bridge pier construction. Current literature lacks substantial experimental data on this specific aspect, demanding urgent attention.

Considering these gaps in knowledge, this paper aims to provide a summary of existing experimental studies regarding the nonlinear cyclic flexural response of circular bridge piers. Additionally, it presents recent experimental findings from the University of Southampton, addressing the critical need for understanding the behaviour of corroded circular columns subjected to cyclic loading. This research fills a significant void in current knowledge, contributing essential insights to enhance the safety and longevity of vital bridge structures.

2. Summary of experimental testing on circular corroded RC columns

In highway bridges, piers are typically positioned in the central reserve, exposing the end regions of these piers to elevated corrosion risks. This heightened susceptibility is a result of de-icing salt splashes from adjacent roads or the downward flow of water carrying chloride ions due to deck expansion joint failures (Kashani et al. 2019). This issue is especially critical in seismic zones, where the lower sections of bridge piers (or both ends in integral bridge piers) are located where plastic hinges are formed during earthquake excitation. Consequently, experimental tests on corroded bridge piers have predominantly focused on cantilever columns, corroding either the entire column or specifically targeting the lower region.

Aquino and Hawkins (2007) conducted experiments on six RC columns. Among them, one served as an uncorroded control specimen, another as a corroded control specimen without reinforcement, and four were reinforced using CPRP sheets. The columns underwent accelerated corrosion procedures, with only the 1200mm immediately above the base corroded. In these columns, significant rust accumulation on the concrete surface and uniform staining of corrosion along the longitudinal reinforcement's length were observed. Column 1 exhibited severe cracking and rust accumulation, mainly due to a large crack opening at the column-base connection, caused by bar slippage. The uncorroded specimen experienced damage primarily due to insufficient lap splice lengths, leading to major cracks parallel to the longitudinal reinforcement upon reaching maximum load. However, the corroded, unreinforced column displayed a distinct failure mode, characterized by buckling of the vertical reinforcement in compression. This was a consequence of tie reinforcement fracturing due to pitting corrosion, leading to loss of confinement and premature buckling of the corroded vertical reinforcement (Aquino and Hawkins, 2007).

Ma et al. (2012) conducted experiments on thirteen columns with varying corrosion levels and axial force ratios. The specimens, subjected to accelerated corrosion, comprised 260mm diameter, 1000mm long columns cast into a 1300mm×360mm×400mm base. Eight out of thirteen columns had axial force ratios below 0.5. Control specimens exhibited flexural failure, with diagonal cracks appearing due to increased lateral load, culminating in core concrete crushing. Corroded specimens displayed similar flexural failure mechanisms but were considerably more brittle. As corrosion and axial load ratio increased, the spacing of cracks at failure widened, and cover concrete spalled at the column's base. Buckling of longitudinal bars and core concrete crushing followed, leading to decreased energy dissipation capacity and ductility. The extent of corrosion proved to be the dominant factor influencing hysteretic behaviour, with severely corroded specimens exhibiting significantly degraded responses (Ma et al., 2012).

Yuan et al. (2017) conducted tests on eight circular RC columns with varying corrosion rates, subjected to repeated axial and cyclic lateral loading. Corrosion rates ranged from 5% to 10%. Results indicated a substantial adverse impact on the columns' capacity due to corrosion. Unexpectedly, vertical axial loading did not significantly affect the yield strength and ultimate capacity of the tested specimens. Finite element analysis revealed a 35% decline in yield strength and a 34% reduction in ultimate displacement for corrosion-damaged columns (Yuan et al., 2017).

3. Experimental testing programme

3.1 Test specimens

Three circular reinforced concrete (RC) columns, each having a diameter of 400mm and a height of 1600mm above the foundation, were designed in accordance with Eurocode 2 standards (CEN 2004). The cross-section of these columns comprised nine vertical bars with a diameter of 16mm. Among these columns, two were specifically detailed for seismic loading as per Eurocode 8 guidelines (CEN 2005), featuring tie reinforcement spaced at 80mm intervals. The third column, designed to match the flexural capacity of the others, followed Eurocode 2 specifications but was not detailed for seismic loading, having a tie reinforcement spacing of 200mm. This column represents an outdated bridge design that does not conform to current codes, characterized by light confining reinforcement. The cover concrete thickness was 30mm, and the concrete utilised had a maximum aggregate size of 10mm. Refer to Figure 1 for the column specimens' detailed configurations, and Tables 1 and 2 are summarising the experimental test matrix and corresponding concrete strength and mechanical properties of reinforcing steel.

3.2 Accelerated Corrosion

To replicate the natural corrosion process of reinforced concrete (RC) structures within a laboratory setting, various simulation methods have been explored in prior studies, including external current techniques, pre-admixed chlorides, and cyclic wetting, and drying. In this research, the authors employed an accelerated corrosion procedure, previously utilized in their own studies, involving the use of external currents. This method establishes an electrochemical circuit using an external power source, where the embedded reinforcing bars act as the anode, and an external material serves as the cathode (commonly made of materials like copper, stainless steel, or regular carbon steel). An electrolyte, usually a saline solution, facilitates the flow of ionic current from the embedded reinforcement to the external cathode. In this experiment, stainless steel plates were used as the external cathode, paired with a 5% sodium chloride (NaCl) saline solution.

The accelerated corrosion process lasted eight and six weeks for columns A1 and B1, respectively, with an average current of 5A applied. After this period, the columns displayed visible surface cracks, both horizontal and vertical. The vertical cracks were a result of the corrosion of longitudinal/vertical reinforcing bars, while the horizontal cracks were due to the corrosion of horizontal hoop/tie reinforcements.

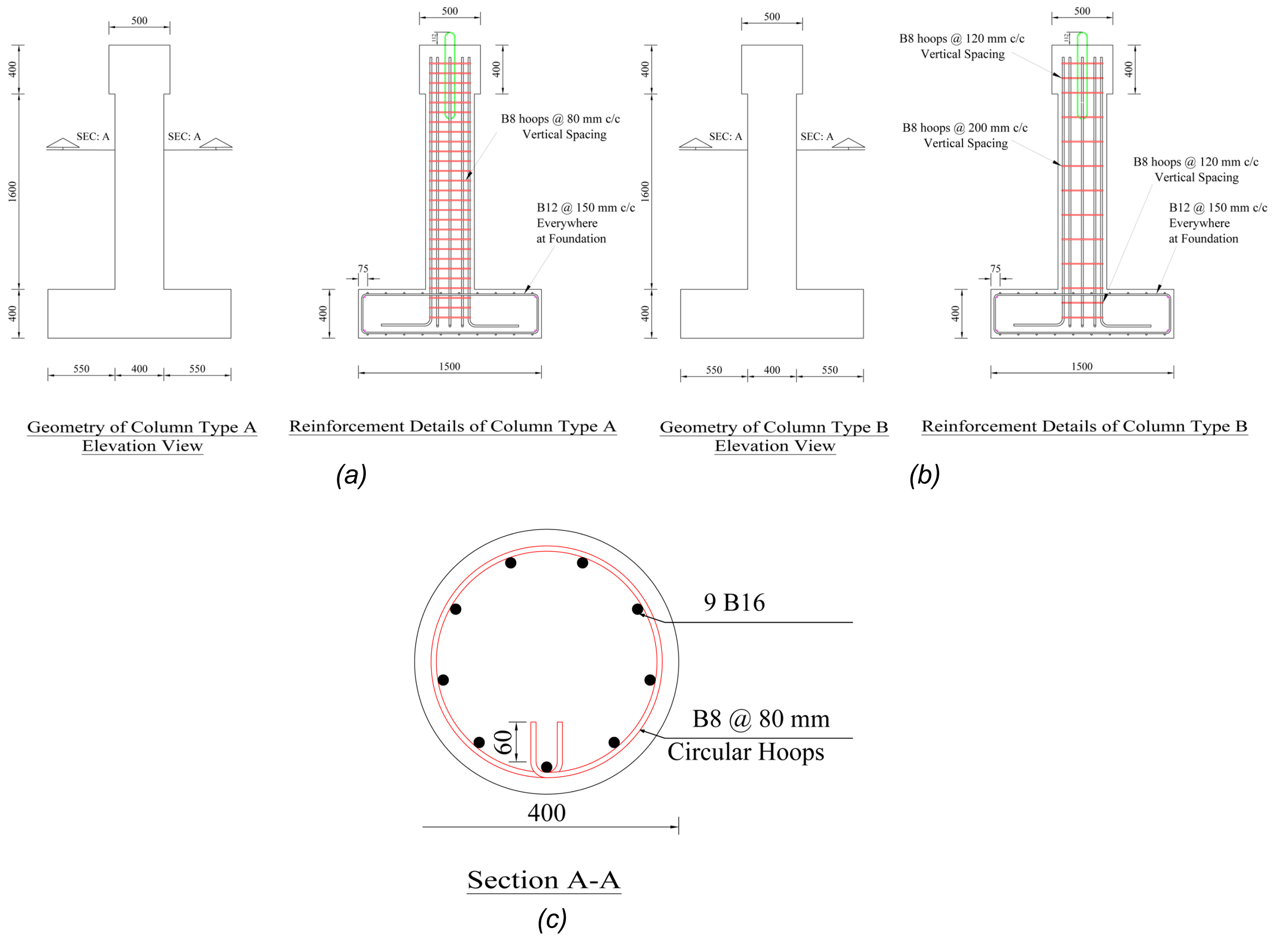

Figure 1. Experimental test specimens: (a) dimensions and reinforcement details of column A, (b) dimensions and reinforcement details of column B, and (c) cross section of columns A and B – all dimensions are in mm.

Table 1 Experimental Test Matrix

Column ID	Design	28 Days Cube Mean Strength	Estimated Mass Loss
Column A	Well-Confined	75.4 MPa	0
Column A1	Well-Confined	73.7 MPa	20%
Column B1	Lightly-Confined	62.6 MPa	20%

Table 2 Mechanical properties of uncorroded steel reinforcement

Reinforcement Type		8mm (B8)	16mm (B16)
Yield Strength	f_y (MPa)	520	530
Modulus of Elasticity	E_s (MPa)	200426	193913
Yield Strain	ε_y	0.00261	0.00273
Ultimate Tensile Strength	f_u (MPa)	645	640
Strain at Ultimate Tensile Strength	ε_u	0.057	0.165
Fracture Strain	ε_f	0.152	0.227
Unit Mass	m (kg/m)	0.396	1.579

3.3 Experimental test setup

A specially designed testing apparatus, located at the Large Structures Testing Laboratory (LSTL) in the University of Southampton, was employed for subjecting large-scale structural components to lateral cyclic loading. The setup featured a 250kN capacity MTS actuator with a 250mm stroke to apply lateral cyclic loading. The columns underwent lateral displacement only, without any axial load. To ensure stability during testing, the reaction frame and foundation block were securely anchored to the laboratory floor using pre-tensioned steel rods. Lateral displacement, ranging from 1.6mm to 96mm, was applied at the top of the column, following a displacement-controlled loading scheme illustrated in Figure 5. Each lateral deformation level underwent 2 repeated cycles. Positive and negative values were assigned to lateral displacements away from and towards the reaction frame, respectively. The testing instrumentation included 5 Linear Variable Differential Transformers (LVDTS) to measure column displacement at different heights. Additionally, Digital Image Correlation (DIC) was employed to capture full-field strain in the plastic hinge region of the columns.

4. Results and analysis from experiments

Figure 2a displays the nonlinear cyclic behaviour of Column A before corrosion, with the corresponding failure points highlighted. In Column A, flexural cracks, caused by reinforcement yielding, emerged at around 1.5% drift. By 2% drift, signs of reinforcement slip and strain penetration at the column base became evident, indicated by splitting at the column base to foundation connection. At 3% drift, the concrete cover began to crush at the column's front face, escalating to significant buckling of vertical reinforcing bars at 4% drift. The buckling initiated at lower drift due to concrete cover crushing at 3%, leading to subsequent concrete cover spalling. Following severe bar buckling, the first buckled bar fractured at 4.5% drift. Finally, during reloading from compression to tension at 5.5% drift, the second buckled bar fractured at 4.5% drift. Notably, the buckled bars fractured during the unloading phase while still under compression, a result of significant inelastic buckling and low-cycle fatigue. The experiment revealed that the interaction between hoop reinforcement stiffness and vertical bar flexural rigidity is crucial in seismic detailing of RC columns, a factor not explicitly considered in the current design codes (e.g., Eurocode 8), indicating a need for further research.

Figure 2b illustrates the nonlinear cyclic response of corroded Column A1. In Column A1, the corrosion primarily affected the bottom of the column, leading to localized damages. At approximately 2% drift, vertical bar slippage and delamination of the column foundation interface occurred, akin to Column A. Unlike the non-corroded column, Column A1 experienced concentrated deformation at its base, with fewer flexural cracks observed during cyclic tests. As the drift ratio increased, concrete cover spalled at about 3% drift, followed by the fracture of the first and second vertical bars at 3.5% drift. Finally, the third vertical bar fractured at around 4% drift, resulting in complete column failure. This distinctive failure mode was caused by localized corrosion in a few vertical reinforcement bars at the column's base. Corrosion measurement data shows that the average corrosion of vertical bars within 200mm above the foundation was 10.40%. However, some of the bars exhibited localised corrosion rates of 17.77%, 19.11%, and 12.03%, respectively, leading to premature fractures at the base of the column.

Figure 2c illustrates the nonlinear cyclic behaviour of corroded Column B1, with failure points marked. The first visible flexural cracks emerged at around 0.5% drift, characterised by a vertical crack along a corroded bar. This crack was a result of pre-existing corrosion, widening during the test. At approximately 0.8% drift, premature spalling of the concrete cover occurred on the column's back face, around 400mm above the foundation, due to prior corrosion (Figure 15a). By 2% drift, the first vertical bar fractured due to severe pitting corrosion, accompanied by concrete cover spalling during load reversal from tension to compression (Figure 15b). Bar buckling became evident at 3% drift, followed by core concrete crushing in the subsequent cycle at 3.5% drift. At 4% drift, a corroded hoop fractured, leading to further core concrete crushing. Notably, localised, and severe corrosion occurred at 400mm above the foundation, where the first vertical bar fractured. This corrosion caused a complete loss of hoop reinforcement, resulting in premature concrete cover spalling.

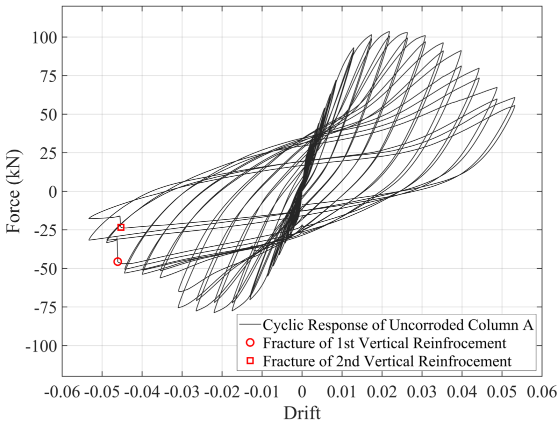

(a)

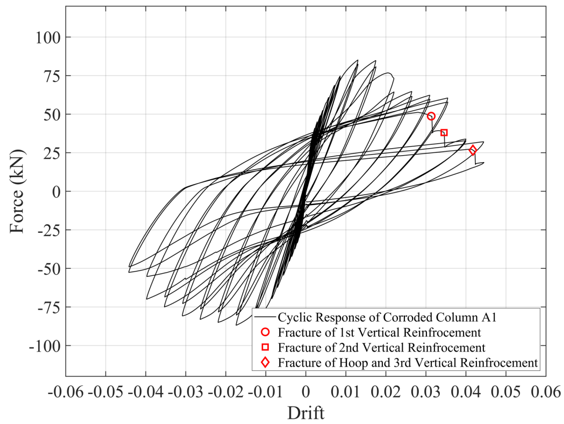

(b)

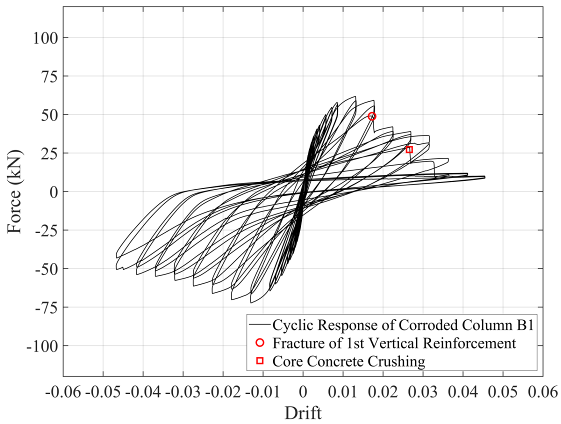

(c)

Figure 2. Nonlinear cyclic response of tested columns: (a) columns A, (b) column A1, and (c) column B1

4.1 Influence of corrosion on effective stiffness of the tested columns

The equation (1) allows for the calculation of the effective secant stiffness of the columns during each cyclic loop.

$$\boldsymbol{K_{sec}} = \frac{|F^{+}_{max,i}|+|F^{-}_{max,i}|}{|\delta^{+}_{max,i}|+|\delta^{-}_{max,i}|} \quad (1)$$

where K_{sec} represents the effective secant stiffness of the column in kN/m, $F_{max,i}$ stands for the peak force in both positive and negative directions in kN, and $\delta_{max,i}$ denotes the peak displacement in both positive and negative directions for each loop in meters.

To compare the stiffness degradation across all columns, the calculated Ksec for each loop in every column is normalised to the initial effective stiffness, K_{ses}, of the uncorroded Column A. The normalised K_{sec} values (illustrated in Figure xx) indicate that the initial stiffness of corroded columns remains higher than that of uncorroded columns until cycle number 11, corresponding to less than a 0.5% drift ratio. However, as the drift ratio of the cyclic test increases, the stiffness degradation in corroded columns becomes more pronounced than in the uncorroded column. This escalation is attributed to the extensive concrete damage experienced by corroded specimens under cyclic loading.

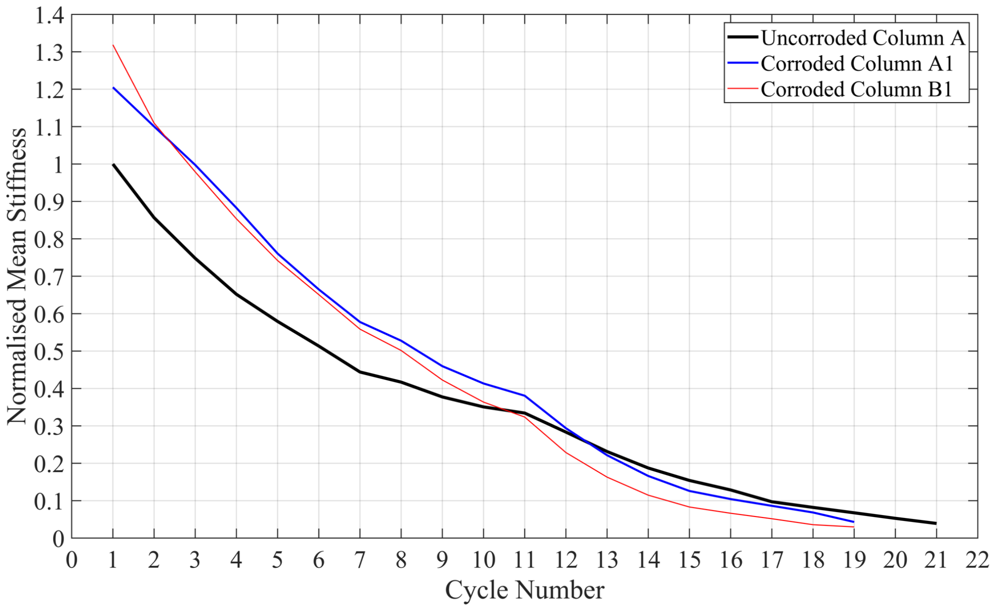

Figure 3. Normalised effective stiffness of all columns

4.2 Influence of corrosion on hysteretic energy dissipation

The energy dissipation capacity, a crucial parameter in earthquake-prone RC bridges, is significantly affected by corrosion, elevating the seismic vulnerability of aging structures. Cumulative hysteretic energy dissipation for each column was normalised to the total dissipated energy during cyclic tests (Figure 4a-c). Energy dissipation remained minimal until cycle 11, consistent with stiffness degradation results in Figure 3. Figure 4(d) compares energy dissipation of corroded and uncorroded columns, highlighting that corroded Column B1 exhibited the lowest capacity due to higher average corrosion and inadequate seismic detailing. Despite Column A1 experiencing the fracture of three bars due to localized corrosion at the base, its average corrosion was lower than that of corroded Column B1. However, Column B1 suffered severe concrete damage and bar buckling due to inadequate confinement. Figure 5 indicates that corrosion significantly impacts ductility and energy dissipation in RC columns, surpassing its effect on residual strength.

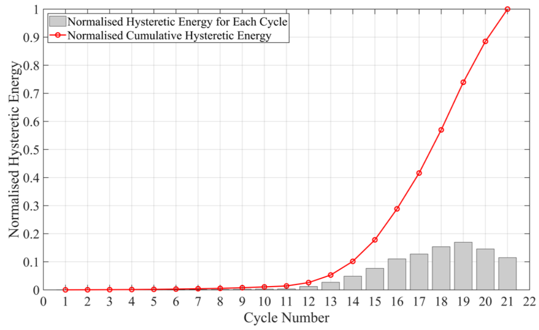

(a)

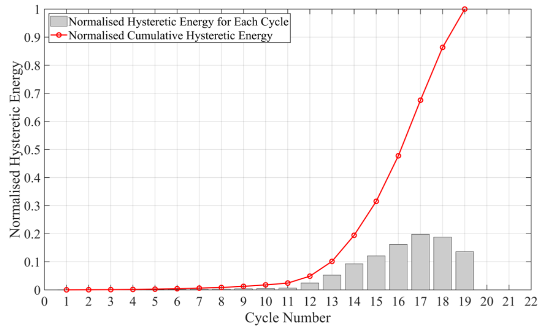

(b)

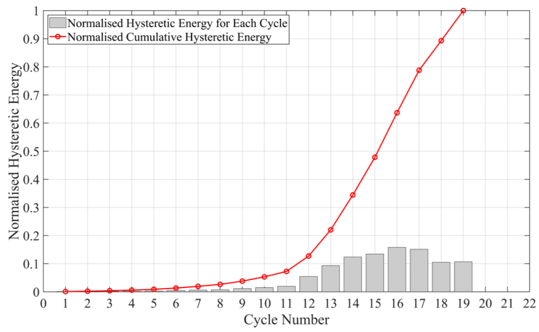

(c)

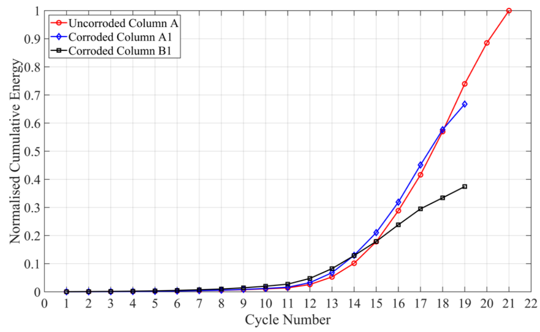

(d)

Figure 4. Hysteretic energy dissipation: (a) Uncorroded Column A, (b) Corroded Column A1, (c) Corroded Column B1, and (d) All columns

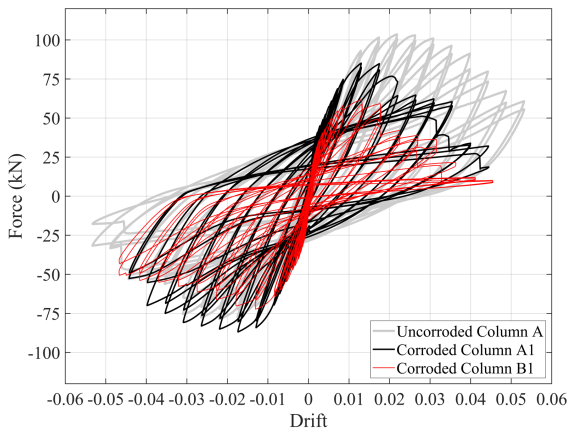

(a)

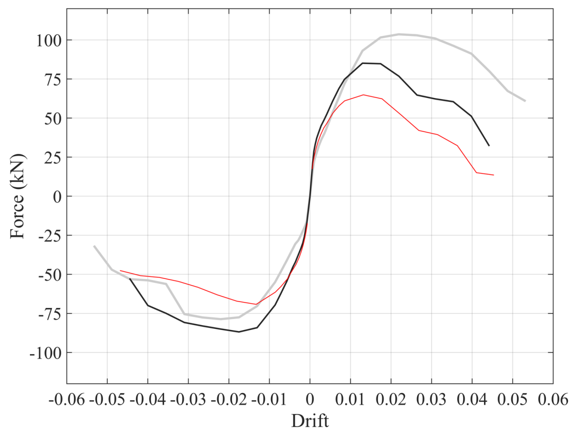

(b)

Figure 5. Nonlinear response of all three columns: (a) cyclic response, and (b) backbone curves

5. Conclusions

A summary of existing experimental research on corroded circular RC columns in flexure is conducted. Furthermore, a summary of experimental results of three circular RC bridge piers with different reinforcement details and corrosion ratios under lateral cyclic loading are presented. The main conclusions of this study can be summarised as follows:

1. The cyclic tests showed that the initial effective stiffness of the corroded columns was more than the uncorroded specimen. However, as soon as drift ratio increased the stiffness degradation of corroded specimens was more significant than the uncorroded specimen.

2. The uncorroded column was seismically detailed according to EC8 criteria. However, significant inelastic buckling followed by low-cycle fatigue fracture of vertical bars was observed. This phenomenon is due to the interaction of hoop reinforcement and vertical bars, which is not explicitly captured in the current seismic design codes. This is an area for further research.

3. Non-uniform corrosion had a significant impact on failure mechanism of corroded specimens. Corrosion in well-confined column A1 was concentrated at the base of the column, and hence, column failure was governed by localised fracture of bars at the base of the column. Corrosion was more evenly distributed in Column B1 with some localised corrosion at about 200mm above the foundation. This has resulted in significant damage in concrete, followed by inelastic buckling and fracture of vertical bars.

4. Corrosion had a more significant impact on ductility and energy dissipation capacity loss than strength loss of corroded columns. The tests results showed that corrosion resulted in about 5% loss of strength in column A1 and 20% loss of strength in column B1. However, it resulted in about 30% reduction in energy dissipation capacity in column A1 and 60% loss of energy dissipation capacity in column B1.

References

Akiyama, M., Frangopol, D. M., Matsuzaki, H. (2011). "Life-cycle reliability of RC bridge piers under seismic and airborne chloride hazards." Earthquake Eng and Struct Dyn., 40: 1671–1687.

Alipour, A., Shafei, B. and Shinozuka, M. (2011). "Performance evaluation of deteriorating highway bridges located in high seismic areas." J Bridge Eng., 6 (5): 597-611.

American Society of Civil Engineers. (2013). Report Card for America's Infrastructure. Retrieved from https://www.infrastructurereportcard.org/a/#p/bridges

Aquino, W., Hawkins, N. M. (2007). "Seismic Retrofitting of Corroded Reinforced Concrete

Columns Using Carbon Composites." ACI Structural Journal., 104(3): 348-356.

Berto, L., Vitaliani, R., Saetta, A., Simioni, P. (2009). "Seismic assessment of existing RC structures affected by degradation phenomena." Struct Saf., 31(4): 284–297.

CEN. (2004). Eurocode 2: Design of concrete structures - Part 2: Concrete bridges - Design and detailing rules (BS EN 1992-2:2005).

CEN. (2005). Eurocode 8: Design provisions of structures for earthquake resistance – Part 2: Bridges (EN1998-2: 2005).

Chiu, C. K., Tu, F. J., and Hsiao, F. P. (2015). "Lifetime seismic performance assessment for chloride-corroded reinforced concrete buildings." Structure and Infrastructure Engineering., 11(3): 345–362.

Choe, D., Gardoni, P., Rosowsky, D., and Haukaas, T. (2008). "Probabilistic capacity models and seismic fragility estimates for RC columns subject to corrosion." Reliab Eng Syst Safe., 93(3): 383–393.

Dizaj, E. A., Padgett, J. E., & Kashani, M. M. (2021). "A Markov chain-based model for structural vulnerability assessmentof corrosion-damaged reinforced concrete bridges." Philosophical Transactions of the Royal Society A, 379(2203), 20200290.

Dizaj, E. A., & Kashani, M. M. (2022). "Nonlinear structural performance and seismic fragility of corroded reinforced concrete structures: modelling guidelines." European Journal of Environmental and Civil Engineering, 26(11), 5374-5403.

Dizaj, E. A., Salami, M. R., & Kashani, M. (2023). "Impact of asymmetrical corrosion of piers on seismic fragility of irregular ageing concrete bridges." Structure and Infrastructure Engineering. https://doi.org/10.1080/15732479.2023.2271887

Ghosh, J., Padgett, J. (2010). "Aging considerations in the development of time-dependent seismic fragility curves." J Struct Eng., 136 (12): 1497–1511.

Kashani, M. M., Maddocks, J., & Dizaj, E. A. (2019). "Residual capacity of corroded reinforced concrete bridge components: State-of-the-art review." Journal of Bridge Engineering, 24(7), 03119001.

Kashani, M., Lowes, L. N., Crewe, A. J., & Alexander, N. A. (2016). "A multi-mechanical nonlinear fibre beam-column model for corroded columns." International Journal of Structural Integrity, 7(2).

Ma, Y., Che, Y., Gong, J. (2012). "Behavior of corrosion damaged circular reinforced concrete columns." Construction and Building Materials., 29: 548-556.

McKenna, F. (2011). "OpenSees: a framework for earthquake engineering simulation." Computing in Science & Engineering., 13(4): 58-66.

Ou, Y. C., Fan, H. D., Nguyen, N. D. (2013). "Long-term seismic performance of reinforced concrete bridges under steel reinforcement corrosion due to chloride attack." Earthq Eng Struct D., 42 (14): 2113–2127.

Rao, A. S., Lepech, M. D., Kiremidjian, A. S., & Sun, X.-Y. (2016a). "Simplified structural deterioration model for reinforced concrete bridge piers under cyclic loading." Structure and Infrastructure Engineering., 13(1): 55–66.

Stewart M.G. (2004). "Spatial variability of pitting corrosion and its influence on structural fragility and reliability of RC beams in flexure." Structural Safety., 2004; 26(4): 453-470.

Vu, N. S., Yu, B., & Li, B. (2016). "Prediction of strength and drift capacity of corroded reinforced concrete columns." Construction and Building Materials., 115, 304–318.

Yuan, Z., Fang, C., Parsaeimaram, M., Yang, S. (2017). "Cyclic Behavior of Corroded Reinforced Concrete Bridge Piers"., Journal of Bridge Engineering., 22(7):1-21.